

Identification of the First Sulfobetaine Hydrogel-Binding Peptides via Phage Display Assay

Ramona B. J. Ihlenburg, David Petracek, Paul Schrank, Mehdi D. Davari, Andreas Taubert,* and Dirk Rothenstein*

Dedicated to the memory of Prof. Wolfgang Meier, a great mentor, colleague, and friend

Using the M13 phage display, a series of 7- and 12-mer peptides which interact with new sulfobetaine hydrogels are identified. Two peptides each from the 7- and 12-mer peptide libraries bind to the new sulfobetaine hydrogels with high affinity compared to the wild-type phage lacking a dedicated hydrogel binding peptide. This is the first report of peptides binding to zwitterionic sulfobetaine hydrogels and the study therefore opens up the pathway toward new phage or peptide/hydrogel hybrids with high application potential.

1. Introduction

Hydrogels are among the most intensely researched materials these days. This is due to their advantageous and highly diverse properties like biocompatibility^[1–4] or useful mechanical properties.^[5,6] Because of this, hydrogels have been explored for numerous fields including medical applications (wound healing, drug delivery, re-mineralization, etc.),^[7,8] soft electronics,^[8,9] or as sensors and actuators.^[10–12]

Zwitterionic hydrogels, a sub-class of the larger family of hydrogels, have attracted attention because of their rather unique

properties and because of their application potential in fields like medical materials,^[13–15] electronics,^[16–18] sensing,^[14,17,19] antifouling surfaces,^[20,21] or materials.^[22,23] For example, Zhang et al. have shown that poly(sulfobetaine) hydrogels are biocompatible, can be implanted, and show properties and responses that are comparable to poly(hydroxyethyl methacrylate) hydrogels.^[24] Similarly, He et al.^[25] showed that poly(sulfobetaine methacrylate) hydrogels support wound healing in mice. Specifically, the authors suggest

that softer and more viscoelastic hydrogels promote effects that are beneficial to wound healing, such as cell proliferation, granulation formation, collagen aggregation, and deposition of chondrogenic extracellular matrix. Zhu et al.^[26] made a dual-functional zwitterionic hydrogel that serves as a glucose sensor, pH sensor, and wound treatment for diabetic patients.


Besides medical applications, zwitterionic hydrogels have, for example, found application as functional soft materials. Jiao et al.^[27] used proline zwitterions incorporated into hydrogels to achieve highly stretchable, yet tough and transparent hydrogels with high stability at temperatures down to -40 °C. They postulate that the resulting materials can be used for wearable electronics and stress sensing. Pei et al.^[28] have shown a similar approach for a strain sensor for wireless monitoring of organ movements. Liu et al.^[29] demonstrated zwitterionic hydrogels with superior antifouling and oil/water separation capabilities. Overall, these examples show the breadth of applications for zwitterionic hydrogels and many more examples can be found in the literature.^[13–23,30,31]

We have previously studied hydrogel scaffolds for biomaterials.^[32–35] In this scope, we have developed a novel sulfobetaine hydrogel based on the new dicationic cross-linker *N,N,N',N'*-tetramethyl-*N,N'*-bis(2-ethylmethacrylate)-propyl-1,3-diammonium dibromide and the sulfobetaine monomer 2-(*N*-3-sulfopropyl-*N,N*-dimethyl ammonium)ethyl methacrylate. The hydrogels and cryogels are effective for removing organic dyes from aqueous solution^[36] and have a rather complex, multi-length scale hierarchical structure.^[37] Overall, hydrogel synthesis is straightforward and, like some of the examples introduced above, these hydrogels could be interesting for application in membranes, antifouling surfaces, or biomaterials. The unique aspect of these hydrogels is that there is a cationic cross-linker, which is different from the more conventional

R. B. J. Ihlenburg, A. Taubert
Institute of Chemistry
University of Potsdam
Karl-Liebknecht-Straße 24–25, D-14476 Potsdam, Germany
E-mail: ataubert@uni-potsdam.de

D. Petracek, D. Rothenstein
Department Bioinspired Materials
Institute for Materials Science
University of Stuttgart
Heisenbergstraße 3, D-70569 Stuttgart, Germany
E-mail: dirk.rothenstein@imw.uni-stuttgart.de

P. Schrank, M. D. Davari
Department of Bioorganic Chemistry
Leibniz Institute of Plant Biochemistry
Weinberg 3, D-06120 Halle, Germany

 The ORCID identification number(s) for the author(s) of this article can be found under <https://doi.org/10.1002/marc.202200896>

© 2023 The Authors. Macromolecular Rapid Communications published by Wiley-VCH GmbH. This is an open access article under the terms of the Creative Commons Attribution License, which permits use, distribution and reproduction in any medium, provided the original work is properly cited.

DOI: 10.1002/marc.202200896

hydrogels based on ethylene glycol cross-linkers. While these traditional cross-linkers have been extensively studied, there is essentially no information on hydrogels made from our new cross-linker and the study therefore focuses on these new hydrogels.

As relatively little is known about the preferences of these new hydrogels toward biological or bioinspired entities, the current study addresses the seemingly simple question of whether there are certain peptide sequences that preferentially interact with these sulfobetaine hydrogels cross-linked with the new, dicationic cross-linker. Knowing these peptides and their binding characteristics to the hydrogel may then 1) enable the construction of soft hybrid materials (e.g., sensors or actuators), 2) allow for an optimized design strategy yielding an improved interaction between hydrogel and surrounding (biological) matrix (e.g., for biomaterials development), or 3) open up new pathways for phage-based therapies.^[38,39]

The phage display method, initially described in 1985,^[40] is a key technology to identify binding peptide sequences for different organic and inorganic materials. Nowadays, it is a high-throughput screening method for protein–protein interactions in molecular biology. In short, genetically manipulated bacteriophages (phages) display pseudo-randomized protein fragments (peptides) as fusion proteins on the phage surface. The selection of peptides is based on the specific interaction of the peptide/phage with a target substrate. The phage links the phenotype (peptide) and the genotype (genetic code) and thus the information on the binding peptide can be easily extracted from the phage DNA. M13 phages have a fiber-like proteinaceous capsid of 900 nm length and 6 nm diameter that encapsulates a single-stranded (ss) DNA genome, encoding five structural proteins and six proteins for replication and assembly.^[41] The major coat protein pVIII builds the phage body with ≈ 2700 copies that are helically arranged around the ssDNA. At the ends of the phage particle the minor coat proteins pIII and pVI at one end and pVII and pIX at the other end are located.^[42]

In recent years, the phage display method has been extended to investigate the interaction between peptides and inorganic materials and thus, binding peptides for different material classes, including semiconductors^[43–45] and metals^[46] have been identified. The selected peptides have been applied in, for example, biomineralization,^[47] stress-resistant materials,^[48] piezo-active nanowires,^[49] bio-sensing platforms,^[50,51] and battery electrodes.^[52,53]

Phage display technology is a method to select peptides based on binding to a target molecule or surface. Therefore, phages are genetically engineered to express an additional peptide fused to a surface protein (coat protein) of the phage. Thereby, each phage clone expresses one individual additional peptide sequence. In the peptide library, 2.7×10^7 different phage clones (and thus the same number of different peptides) are mixed. From this mixture, the phage clones that bind to the target can be selected. The phage has the task of physically connecting the phenotype with the genotype, that is, that the binding peptide (phenotype) and the corresponding DNA (genotype) can be isolated together. The peptide sequence is then deduced from the corresponding DNA, which encodes the peptide, by DNA sequencing.

Indeed, binding peptides directed against polymers have been selected by phage display. The interaction was at-

tributed to the recognition of tacticity, that is, the position of functional groups in the side chains, the structure, and the crystallinity of the target system.^[54] However, past research mainly focused on hydrophobic polymer systems such as poly(methyl methacrylate) (PMMA),^[55,56] poly(L-lactide),^[57] polyetherimide,^[58] polypropylene,^[59] poly(dimethyl siloxane),^[60] and polystyrene/polyvinyl chloride.^[61] A common sequence for binding peptides has not been identified, but many of the binding peptides were enriched in aromatic and hydrophobic amino acid residues.^[62,63]

In contrast, only a few reports describe peptides binding to hydrophilic polymer systems, charged or uncharged. Poly(propylene oxide), an uncharged polymer, strongly binds to the peptide DFNPYLGVTPL.^[64] A few examples of peptides interacting with hydrophilic and charged systems are published. The peptide HNAYWHWPPSMT binds to poly(2-methoxy-5-propyloxysulfonate-1,4-phenylenevinylene), and the binding was suggested to be due to π – π interactions of tryptophan residues.^[65] Aromatic amino acids, mainly tryptophan, in the peptide sequences are also beneficial for binding to charged polymer nanoparticles.^[66] In addition to aromatic amino acids mediating the binding, peptides with charged amino acid residues, mostly positively charged amino acids, bind to poly(*N*-isopropylacrylamide).^[67]

The current study, therefore, focuses on the identification of peptides binding to our hydrogel based on the new cross-linker.^[36,37] Since, to the best of our knowledge, this work is the first report on sulfobetaine hydrogel-binding peptides, we will discuss similarities and differences with peptides interacting with non-sulfobetaine hydrogels.^[64,68] The study further expands the pool of hydrogel-binding peptides to sulfobetaine hydrogels and provides a hypothesis on the binding mechanism based on computer analysis that opens avenues to next generation multifunctional soft materials.

2. Results

2.1. Phage Display

Sulfobetaine hydrogel-binding peptides were selected from a random 7- and 12-mer peptide library by phage display (Table 1 and Tables S1 and S2, Supporting Information). Phage clones expressing the binding peptides were analyzed after the fourth and fifth bio panning rounds. Eight different 12-mer peptides were identified from 50 phage clones. The 7-mer peptides showed greater diversity; here, 20 different peptide sequences were isolated from 45 phage clones.

In the case of the 12-mer peptides (Table 1), the peptide LLADTTHRPWT clearly prevailed over other sequences with 40 out of 50 phage clones expressing this sequence. Besides this sequence, seven other sequences were isolated. The phage clones expressing 7-mer peptides were more diverse, with 20 different peptide sequences identified. The most frequent sequence was HGGVRLY with an occurrence of 8 out of 45. However, the selection frequency of a peptide does not necessarily correlate with the binding strength of a peptide.

The change in the abundance of individual amino acids in the entirety of the selected peptides compared to the initial peptide library is an indicator of the importance of individual amino acids

Table 1. Peptides binding to sulfobetaine hydrogels. 7- and 12-mer peptide sequences which were applied in phage-based binding assays. In total, 20 different 7-mer peptide sequences from 45 phage clones and 8 different 12-mer peptide sequences from 50 clones were identified. Peptide sequences are in single-letter amino acid code. Color code: red: positively charged aa, blue: negatively charged aa, yellow: tryptophan. The peptide sequences are sorted according to their length and calculated isoelectric point (pI). The strongest binding peptides are printed bold.

Peptide #	Sequence	Length	Frequency	pI
18	QQTN W SL	7	4/45	5.50
107	QLAVAPS	7	4/45	5.50
56	GQSEKHL	7	6/45	7.19
26	KIAVIST	7	5/45	8.88
48	TVNFKLY	7	3/45	8.88
46	HGGVRLY	7	8/45	9.06
4	VPTF W TKIEHAA	12	1/50	7.19
7	LLADTTHHRP W T	12	40/50	7.38
80	NR P DSAQ F WLHH	12	3/50	7.38
14	TMGFTAPRPFHY	12	1/50	9.06

for binding to the target substrate is (Table 2). The quotient of the amino acid frequency in the hydrogel-binding peptides and in the initial peptide library is indicative of enriched (criterion: quotient > 1.25) or depleted (criterion: quotient < 0.75) amino acid residues. Enriched amino acid residues may have a beneficial effect on the binding of peptides, while depleted amino acid residues might have an adverse effect on the interaction. For both peptide lengths, 7- and 12-mer peptides, positively charged amino acids were enriched while negatively charged amino acids were depleted. Furthermore, aromatic amino acids with a heterocyclic indole may also favor the peptide–hydrogel interaction.

A phage-based binding assay was performed to estimate the binding strength of individual peptides (Figure 1). Since not all clones could be tested, a selection was made (Table 2). The choice of the 12-mer peptides included the two most abundant peptides. In addition, two peptides were chosen that differed significantly in their isoelectric point. For the 7-mer peptides, the six most frequently occurring peptides were selected. The binding strength of the peptides was determined in parallel to wild-type phages, that do not express a binding peptide, as negative control. This allows for an exclusion of possible contributions to the interaction from the phage itself. Furthermore, no changes in the peptide sequence or hydrogel composition has to be made. The

Table 2. Frequency of amino acid residues of hydrogel-binding peptides. The frequencies are given as quotients of the amino acid frequency in the selected peptides, and the initial peptide library (NEB), that is, numbers >1 indicate enrichment and numbers <1 indicate depletion of the amino acid. Each peptide sequence was considered only once for the calculation of amino acid abundance, regardless of its number of occurrences in the peptide pool. The threshold value for enriched and depleted amino acids was set to 1.25 and 0.75, respectively. Enriched amino acid residues are highlighted in dark grey and depleted amino acid residues are highlighted in light grey. Amino acids are indicated in one-letter code.

Peptide length	Basic		Small			Hydrophobic				Acidic			Amide		Nucleophilic		Aromatic			
	H	K	R	G	A	V	L	I	P	M	D	E	N	Q	S	T	C ^{a)}	Y	F	W
7-mer	0.78	1.30	0.87	1.06	1.81	1.00	0.85	1.05	0.63	0.77	0.33	0.58	1.26	1.02	1.05	1.46	0.00	0.66	1.06	1.95
12-mer	1.98	1.49	1.48	2.14	2.08	0.71	1.64	0.41	1.48	1.07	0.99	0.44	0.91	0.54	0.97	1.25	0.00	0.77	1.68	3.16

^{a)} The abundance of cysteine residues was not considered because cysteine interferes with the infection of bacteria and phage formation, therefore the values may not be based on binding.

phage-based binding assay also showed no direct correlation between the frequency of isolation of a phage clone and the binding strength of the peptide.

The abundance of a particular peptide sequence cannot be directly equated with the binding strength, since only a random sample of the isolated phage clones was sequenced and biological factors, such as the infectivity of a clone, may also influence the abundance. The values of the binding strength were normalized to M13 wt that did not express an additional binding peptide (wt phage titer = 1). Four peptides showed a significantly higher binding strength compared to the wt phage. The binding strength of the 7-mer peptides 56 and 18 was increased by a factor of 3, and doubled for the 12-mer peptides 4 and 80. Two 7-mer peptides (107, 26) and the 12-mer peptide 7 showed a binding strength similar to the wt phages. Only three peptides (7-mer: 46, 48; 12-mer: 14) showed poorer binding compared to the wt phages.

To explain the experimentally observed trends in the binding strengths, electrostatic potential map analyses were carried out for all peptides. First, 3D models for the respective peptides were generated using the AlphaFold2 software.^[69] The generated peptide models were relaxed using the AMBER14 force field^[70] and afterward scored using IDDT values.^[71] The peptide models generally showed good IDDT values (see Table S3, Supporting Information), indicating reliable peptide models, suitable for further analyses.

The predicted structures show that the propensity of most peptides to adopt a defined structure is very weak. This possibly suggests that the binding strength correlates with the electrostatic potential exhibited by the peptides. To confirm this, we generated electrostatic potential surfaces for all peptide models using the Adaptive Poisson–Boltzmann Solver (APBS).^[72] To visually contour the potential charges on the surface a three-color red (−1), white (0), and blue (+1) scale APBS was rendered in PyMOL, coloring negatively, neutrally, and positively charged patches in red, white, and blue, respectively (Figure 2 and Figure S1, Supporting Information).

As a general trend, the electrostatic potentials showed that most peptides, excluding 12-mer peptide 7, display a polarized distribution of charges. One side of the peptide contains a positive patch and the other side contains a negative patch, separated by a neutral zone of variable size (Figure 2A,B).

A closer look at the electrostatic potential surface for the hydrogel-binding peptides showed that this charge distribution could be also observed in almost all selected peptides (see Table S3, Supporting Information). As a result, it is highly likely that

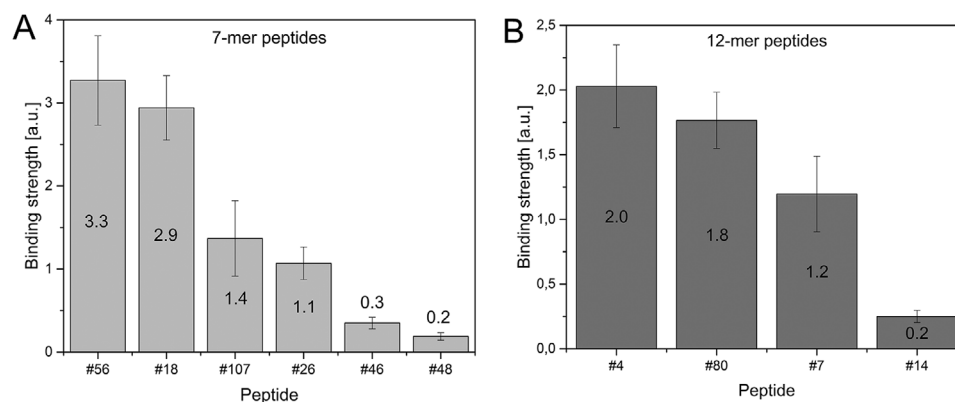


Figure 1. Relative binding strength of selected peptides to sulfobetaine hydrogels. The binding strength is normalized to the wild-type (wt) phage not expressing an additional peptide. A) 7-mer peptides provide up to threefold higher binding strength. B) 12-mer peptides show up to twofold higher binding strength to the hydrogel than the wt.

this polarization of the electrostatic potential is essential for the effective binding of the peptide to the hydrogel through one side without having repulsive effects from the opposite charge (see Figures S1 and S2, Supporting Information). In the case of the 12-mer peptide 7, two distinct positive and negative patches were flanked by one another (Figure 2B), suggesting repulsive effects that affect the binding and lead to a decrease in the overall binding strength.

Second, the electrostatic potentials also displayed peptides containing larger negative patches, correlating with higher binding strength to the hydrogel overall. Coupled with this observation (that peptides with pI at neutral to slightly acidic pH values also show better binding strength than their basic counterparts) it can be assumed that binding predominately happens through the negatively charged regions of the peptides.

In addition, a positively charged peptide stretch is also necessary for a strong interaction. Again, 12-mer peptide 7 is an outlier from this observation, as it contains two relatively large negatively charged patches while exhibiting a relatively small binding strength of 1.2 (Figure 2B). This decreased binding strength is to be expected, as the negatively charged binding regions are flanked by positively charged regions, resulting in partially repulsive effects.

3. Discussion

To our best knowledge, sulfobetaine hydrogels have never been studied in phage display experiments before. We succeeded in the selection of peptides, which bind to the zwitterionic hydrogel and identified some preliminary design principles of such zwitterion hydrogel-binding peptides.

In general, the large majority of peptides contain charged amino acids. The amino acids often occur in so-called doublets, tandems of positively and negatively charged amino acids. Such doublet formation often occurs in proteins that are related to biomineralization.^[74] Doublets were also found in 7-mer peptides. In addition, positively charged amino acids were often found in the identified peptide sequences. As shown for inorganic-binding peptides,^[44] the amino acid histidine is also

significantly enriched in peptides that interact with the sulfobetaine hydrogels.

Beside charged amino acids, the abundance of the aromatic amino acid residues of the selected peptides changes significantly compared to the starting peptide library. While tyrosine and phenylalanine were depleted in the selected hydrogel-binding peptides, tryptophan was highly enriched and present in the majority of peptides with the best binding properties.

This is a rather interesting observation, as the hydrogel is charged and has an overall positive charge stemming from the cross-linker. We currently speculate (as there are no real possibilities of π - π interactions in the hydrogel) that the strong enrichment and consequently effective binding of tryptophan units could be due to hydrogen bonding between the nitrogen atom in the tryptophan side chain and the peptide (possibly, the water molecules in the hydrogel are strongly involved in this process). Molecular simulation-based materials informatics also suggest that tryptophan plays a central role in the binding of peptides to PMMA hydrogels.^[75] The binding affinities (binding free energies) were obtained with molecular simulations based on the response surface method (Kriging method). There, the calculated detachment energies of tryptophan from COOCH₃ and CH₃ were the highest of the biogenic amino acids.

All peptides with good binding properties to the sulfobetaine hydrogels (12-mer peptides 4, 80, 7, and 7-mer peptides 56, 18, 107, 26; Figure 2) have a calculated negative charge at pH 7.5 between -0.2 and -0.1 (in spite of the fact that most peptides are enriched in basic, i.e., positively charged amino acid residues). This indicates that the main binding mode may be strongly driven by electrostatics because the hydrogel has a positive overall charge.

The reason is as follows: the SPE monomer carries one positive and one negative charge, hence is neutral overall. However, the cross-linker carries two positive charges, see refs. [36, 37]. As stated in the experimental part, the hydrogel synthesis starts with 12 mmol of the SPE monomer and 1.2 mmol of the cross-linker, yielding a 10:1 molar ratio of monomer:cross-linker. Assuming full conversion (which is, however, highly unlikely), there would be 12 mmol of ammonium groups and 12 mmol of sulfonate groups (both from the SPE monomer) in the final hydrogel, and this would effectively lead to a net charge neutralization.

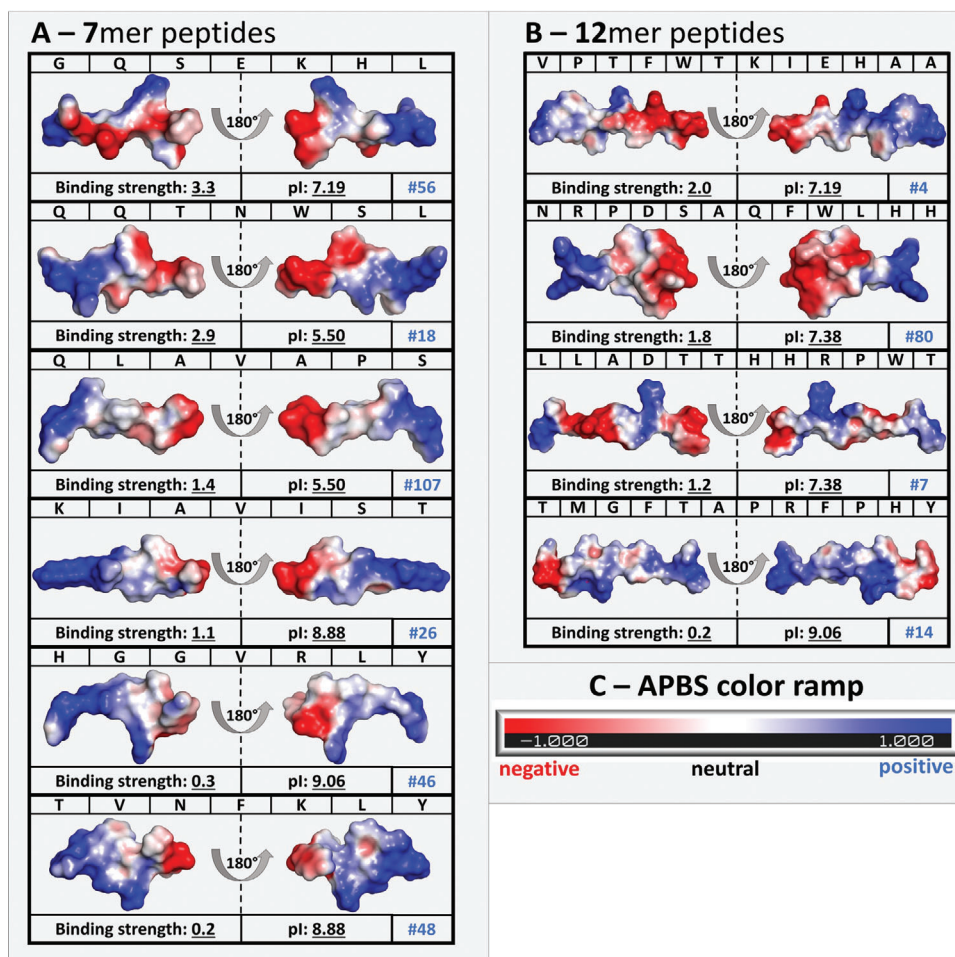


Figure 2. Comparison of electrostatic potential surfaces for models of 7-mer peptides 56, 18, 107, 26, 46, and 48, and 12-mer peptides 4, 80, 7, and 14. The charge maps for representation of the electrostatic potential surfaces were calculated using the Adaptive Poisson–Boltzmann Solver (APBS) software^[72] as a Python package imported for PyMOL2 software.^[1] The distributions of the charges were mapped on the molecular surfaces of the peptides model and contoured based on the APBS coloring scale rendered within PyMOL. Negatively charged surface patches are shown in red, neutrally charged surface patches in white, and positively charged surface patches in blue. The surfaces are shown from two views of the same perspectives, related by a 180° rotation around a vertical axis. A) Amino acid sequence, binding strength, isoelectric point, and electrostatic potential surfaces for the 7-mer peptides 56, 18, 107, 26, 46, and 48 ordered from top to bottom by decreasing binding strength. B) Amino acid sequence, binding strength, isoelectric point, and electrostatic potential surfaces for the 12-mer peptides 4, 80, 7, and 14 ordered from top to bottom by decreasing binding strength. C) APBS coloring scale for contouring electrostatic potential charges on the molecular surface of the peptide models. The scale consists of a three-color red (–1)—white (0)—blue (+1) code for coloring of negative, neutral, and positive patches, respectively.

However, there is also 1.2 mmol of the cross-linker, and as each cross-linker molecule carries two positive charges, there is 2.4 mmol of positively charged units in the hydrogel at full conversion. This excess positive charge is very likely a key source for the peptide/hydrogel interaction. In addition, hydrogen bonding, dipolar interaction, and further ionic interactions between both the ester groups in the polymer backbone and the peptide and between the charged entities of the SPE monomer and the peptides are further sources of interaction.

It must, however, clearly be stated at this point that this charge distribution can drastically change at different pH. Lower pH values will significantly drive up the degree of protonation on the basic amino acid residues in the peptides and, consequently, also lead to a protonation of the carboxylate groups in the acidic residues. As a result, there will be situations, where the patches as

shown in Figure 2 will not carry their specified charge anymore. Negatively charged patches can turn neutral due to protonation of the carboxylates and some of the unprotonated nitrogen atoms in the basic residues can further be protonated. This will then potentially lead to a repulsive interaction between a positively charged cross-linker and a positively charged peptide residue. Based on our findings and the visualization of the surface electrostatic potential, we can conclude preliminary design principles for sulfobetaine hydrogel-binding peptides.

Three categories of binding strength (strong, medium, low) were distinguished based on the molecular properties of the peptides: 1) strong binders have adjacent positive and negative stretches, which are not separated by other amino acid residues (peptides 56, 18, 4, and 80). 2) Medium binders have the charged peptide stretches separated by a stretch of neutral amino acids

(peptides 107, 26, and 7). 3) Finally, peptides, showing limited binding capacity only have a small positively charged region on an otherwise negatively charged peptide surface (peptides 46, 48, and 14).

Although we therefore postulate that one of the main driving forces for peptide–hydrogel interaction is a negative electrostatic potential surface, positive charges seem to be necessary for an effective peptide binding, too. Positively charged amino acids can balance the charges of the bound peptide, resulting in a stable binding. Moreover, positively charged amino acids may interact with unreacted sulfobetaine residues of the hydrogel. Furthermore, peptides with flexible and large side chains in the negative patches are better binders; this is visible from the computational analyses. Larger side chains allow for more flexibility of the peptide and thus a better occupancy of suitable binding sites in the hydrogel. The superiority of a flexible peptide ligand may also reflect the structure of the hydrogel with fluctuations and disorder on small size scales that can be overcome by flexibility.

4. Conclusion

The current study is the first binding assay of peptides to sulfobetaine hydrogels. The hydrogels are unusual because they do not use a traditional, commercial cross-linker. The combination of phage display and computational analysis clearly provides a first glimpse into how rather short and essentially disordered peptides interact with sulfobetaine hydrogels. Overall, the data show that phage display analysis coupled with computational analysis can 1) be used to elucidate why and how certain peptides bind to sulfobetaine hydrogels and 2) provide inspirations for the design of new materials or surfaces where the interaction can be tuned (and possibly alternated between an ON and OFF state) by way of the specific peptide sequence. Potential applications are phage-reinforced hydrogels, hydrogels with specific sensing properties provided by the phages, materials for affinity chromatography, or materials for soft robotics that react to multiple stimuli. Furthermore, peptide/polymer hybrids have been suggested for separating biomacromolecules, where one specific peptide adheres to, for example, a polymer hydrogel particle while others do not⁽⁶⁶⁾ resulting in the separation of bio(macro)molecule by selective adsorption for various analytical purposes.

5. Experimental Section

Materials: Yeast extract, tryptone, agar, EDTA, NaCl, polyethylene glycol (PEG)-8000, PEG-8000/sodium chloride (PEG/NaCl), Tris, Tween 20, glycine, bovine serum albumin (BSA), HCl (37%), isopropyl- β -D-thiogalactopyranoside, 5-bromo-4-chloro-3-indolyl- β -D-galactopyranoside (Xgal), E.Z.N.A. M13 DNA Mini kit (Omega Bio-tek, USA), Monarch Plasmid miniprep kit (New England Biolabs, USA), and phage libraries (Ph.D.-12 Phage Display Peptide Library and Ph.D.-7 Phage Display Peptide Library, New England Biolabs, USA), were purchased as p.a. quality from Roth, Sigma-Aldrich, and Merck, and used without further purification.

The monomer 2-(dimethylamino ethyl)methacrylate (stabilized with hydroquinone monomethyl ether for synthesis, Merck), 1,3-dibromo propane (98%, Alfa Aesar), dimethyl formamide (water < 150 ppm, VWR Prolabo), acetone (VWR, GPR RECTAPUR), *tert*-butyl methyl ether (99%, Alfa Aesar), 2-(*N*-3-sulfopropyl-*N,N*-dimethyl ammonium) ethyl methacrylate (SPE, Merck), and potassium peroxodisulfate (\geq 99%, Fluka Analytical) were used without further purification.

Hydrogel Synthesis: The cross-linker TMBEMPA/Br and the hydrogels were synthesized as published.^[37] In short, TMBEMPA/Br (1.2 mmol, 0.6196 g) and the monomer SPE (12 mmol, 3.3525 g) were dissolved in 7.2 mL of distilled water. This mixture was purged with N₂ for 30 s. Then KPDS (0.09 mmol, 24 mg) was added. Subsequently, 3 mL of this parent solution were transferred to a 20 mL polypropylene container with a twist-off-cap (Samco™ Bio-Tite™ Specimen Containers, Thermo Scientific) with an Eppendorf pipette. Before the containers were closed, the liquid was purged again with N₂ for 10 s. The containers were placed in a compartment drier (Memmert UF55Plus with grating, closed system setup, ventilation 30%) at 70 °C for 20 min. The resulting, transparent to slightly opaque gels were purified by immersion in 40 mL of ultrapure water (18.5 M Ω cm⁻¹, 1 ppb TOC, 25 °C) for 4 weeks. The structure and properties of the resulting gels were described previously.^[37]

Phage Display M13 p3 Experiments: 7- and 12-mer peptides that specifically bind to the hydrogels were isolated from random peptide libraries by phage display (New England Biolabs, Inc.). The peptide libraries either express 7- or 12-mer peptides as N-terminal fusion protein with the minor coat protein p3 of M13 phages with a short spacer sequence (GGGS) separating the peptides from the p3 coat protein. General phage methods were conducted according to the manufacturer's recommendations.

The hydrogel binding substrates (\approx 5 × 5 × 5 mm³) were incubated at least 1 h in Tris buffered saline (50 mM Tris pH 7.5; 150 mM NaCl) supplemented with 0.1% Tween 20 (TBST). The TBST was removed and 500 μ L of fresh TBST was added to the substrates. Subsequently, 10 μ L of the phage libraries (1 × 10¹³ pfu mL⁻¹, pfu = plaque forming units) were added and the mixtures were incubated at room temperature (RT) under constant agitation (Thermomix, 800 rpm) for 60 min. Unbound phages were removed from the substrate by washing ten times in TBS supplemented with 0.5% Tween 20. The bound phages were eluted for 10 min at RT in 1 mL of glycine elution buffer (0.2 M glycine, pH 2.2 supplemented with 1 mg mL⁻¹ BSA). The eluate was neutralized with 150 μ L of 1 M Tris-HCl, pH 9.1. The eluted phages were amplified in *Escherichia coli* (*E. coli*) ER2738 in a shaking incubator (250 rpm) for 4.5 h at 37 °C. The phages were purified by polyethylene glycol-8000/sodium chloride (PEG/NaCl) precipitation. The phage concentration after this first bio panning round was determined by phage titering. Briefly, 200 μ L of an *E. coli* culture in the exponential growth phase were infected with 10 μ L of the diluted phage suspension and plated onto culture medium. The cultures were incubated overnight at 37 °C. The pfu were counted and calculated on the concentration of the original phage suspension.

In the following bio panning rounds, 1.5 × 10¹¹ phages from the previous bio panning round were applied. To increase the specificity of hydrogel-binding peptides in total five panning rounds were performed. From each experimental set up 30 randomly selected phage clones after the fourth and fifth bio panning round were analyzed by DNA sequencing (BioEdit Sequence Alignment Editor). The peptide properties, that is, isoelectric point (pI) and the charge at pH 7.5, were calculated with Protein Calculator v3.4.

Binding Assay M13 p3 Experiments: The binding strength of individual hydrogel-binding peptides was determined with a phage-based binding assay. Phage clones expressing a hydrogel-binding peptide were amplified in *E. coli* ER2738 and isolated by PEG/NaCl precipitation. Phages were resuspended in an appropriate volume of TBS and the concentration of the phage stocks were determined by UV–vis spectroscopy and phage titering.

For the binding assay, a specific number of phages was incubated with a defined volume of hydrogel in TBS at RT for 1 h. Unbound phages were removed by washing with TBS supplemented with 0.5% Tween 20. Bound phages were eluted with glycine elution buffer. The phage titer was determined by UV–vis spectroscopy and phage titering using appropriate dilutions of the eluted phage suspensions. For the phage titering, only plates with a minimum of 40 pfu were considered in the concentration calculations. Since the infection values were subject to fluctuations, the phage titration was performed four times. The phage titer directly correlates with the binding strength of the hydrogel-binding peptide. To facilitate comparison, the values were normalized to the wild type phages (wt phage titer = n1).

Molecular Modeling: Peptide structures were predicted using AlphaFold2^[69] by inputting the peptide sequences in FASTA formatting and running the algorithm with default settings. The predicted structures (a total of five for each peptide) were relaxed and energy minimized by AlphaFold2 using the AMBER 14.0 force field.^[70] The relaxed models were then scored by AlphaFold2 using IDTT^[71] calculations and ranked accordingly. The best ranked model for each peptide was used for electrostatics calculation with the APBS using the PDB2PQR^[76] and APBS solver^[72] software packages for Python imported in PyMOL2. Protonation states of the amino acid residues were assigned based on PropKa calculations at pH 7.^[77] Generation and analysis of the electrostatic potential surfaces for the peptides was performed using PyMOL2 (Schrödinger) software.^[73] For this, a custom PyMOL script was developed to automatize generation and analysis called “peptide_analysis.pml.” The workflow is described in the Method S1, Supporting Information. Detailed information on the plugin, the code, and how to use it is found on GitHub under “https://github.com/Protein-Engineering-Framework/APBS-peptides.”

Supporting Information

Supporting Information is available from the Wiley Online Library or from the author.

Acknowledgements

The authors thank the University of Potsdam for financial support (A.T., grant 53170000). D.R. was in part supported by the Volkswagen Stiftung under the project “Self-assembled nano-reactors via bacteriophage engineering (ROBOPHAGE),” and the DFG (RO-3965/3-1). D.R. also thanks the University of Stuttgart for support with laboratory infrastructure and space and financial support. M.D.D. is supported through funds from the Leibniz Institute of Plant Biochemistry.

Open access funding enabled and organized by Projekt DEAL.

Author Contributions

The manuscript was written through the contributions of all authors. All authors have given approval to the final version of the manuscript.

Conflict of Interest

The authors declare no conflict of interest.

Data Availability Statement

The data that support the findings of this study are available from the corresponding author upon reasonable request.

Keywords

hydrogels, LLADTTHHRPWT, peptide binding, phage displays, QQT-NWSL, sulfobetaine, surface modifications, TVNFKLY

Received: November 15, 2022

Revised: January 11, 2023

Published online: February 16, 2023

[1] E. Caló, V. V. Khutoryanskiy, *Eur. Polym. J.* **2015**, *65*, 252.

- [2] J. Saroia, W. Yanen, Q. Wei, K. Zhang, T. Lu, B. Zhang, *Bio-Des. Manuf.* **2018**, *1*, 265.
- [3] X. Xue, Y. Hu, Y. H. Deng, J. C. Su, *Adv. Funct. Mater.* **2021**, *31*, 2009432.
- [4] L. L. Palmese, R. K. Thapa, M. O. Sullivan, K. L. Kiick, *Curr. Opin. Chem. Eng.* **2019**, *24*, 143.
- [5] S. Bashir, M. Hina, J. Iqbal, A. H. Rajpar, M. A. Mujtaba, N. A. Alghamdi, S. Wageh, K. Ramesh, S. Ramesh, *Polymers* **2020**, *12*, 2702.
- [6] M. Shibayama, *Soft Matter* **2012**, *8*, 8030.
- [7] S. Correa, A. K. Grosskopf, H. L. Hernandez, D. Chan, A. C. Yu, L. M. Stapleton, E. A. Appel, *Chem. Rev.* **2021**, *121*, 11385.
- [8] J. H. Li, C. T. Wu, P. K. Chu, M. Gelinsky, *Mater. Sci. Eng., R* **2020**, *140*, 100543.
- [9] H. Yuk, B. Lu, X. Zhao, *Chem. Soc. Rev.* **2019**, *48*, 1642.
- [10] J. Shang, X. Le, J. Zhang, T. Chen, P. Theato, *Polym. Chem.* **2019**, *10*, 1036.
- [11] Y. S. Zhang, A. Khademhosseini, *Science* **2017**, *356*, eaaf3627.
- [12] X. Y. Liu, J. Liu, S. T. Lin, X. H. Zhao, *Mater. Today* **2020**, *36*, 102.
- [13] J. Wu, Z. Xiao, A. Chen, H. He, C. He, X. Shuai, X. Li, S. Chen, Y. Zhang, B. Ren, J. Zheng, J. Xiao, *Acta Biomater.* **2018**, *71*, 293.
- [14] L. F. Wang, G. R. Gao, Y. Zhou, T. Xu, J. Chen, R. Wang, R. Zhang, J. Fu, *ACS Appl. Mater. Interfaces* **2019**, *11*, 3506.
- [15] X. Qiu, J. M. Zhang, L. L. Cao, Q. Jiao, J. H. Zhou, L. J. Yang, H. Zhang, Y. P. Wei, *ACS Appl. Mater. Interfaces* **2021**, *13*, 7060.
- [16] X. J. Sui, H. S. Guo, P. G. Chen, Y. N. Zhu, C. Y. Wen, Y. H. Gao, J. Zhang, X. Y. Zhang, L. Zhang, *Adv. Funct. Mater.* **2020**, *30*, 1907986.
- [17] C. J. Lee, H. Y. Wu, Y. Hu, M. Young, H. F. Wang, D. Lynch, F. J. Xu, H. B. Cong, G. Cheng, *ACS Appl. Mater. Interfaces* **2018**, *10*, 5845.
- [18] S. E. Feicht, A. S. Khair, *Soft Matter* **2016**, *12*, 7028.
- [19] W. Yang, H. Xue, L. R. Carr, J. Wang, S. Y. Jiang, *Biosens. Bioelectron.* **2011**, *26*, 2454.
- [20] H. M. Chan, N. Erathodiyil, H. Wu, H. F. Lu, Y. R. Zheng, J. Ying, *Mater. Today Commun.* **2020**, *23*, 100950.
- [21] W. Pan, T. J. Wallin, J. Odent, M. C. Yip, B. Mosadegh, R. F. Shepherd, E. P. Giannelis, *J. Mater. Chem. B* **2019**, *7*, 2855.
- [22] L. D. Blackman, P. A. Gunatillake, P. Cass, K. E. S. Locock, *Chem. Soc. Rev.* **2019**, *48*, 757.
- [23] W. J. Yang, K.-G. Neoh, E.-T. Kang, S. L.-M. Teo, D. Rittschof, *Prog. Polym. Sci.* **2014**, *39*, 1017.
- [24] Z. Zhang, T. Chao, L. Liu, G. Cheng, B. D. Ratner, S. Jiang, *J. Biomater. Sci., Polym. Ed.* **2009**, *20*, 1845.
- [25] H. He, Z. Xiao, Y. Zhou, A. Chen, X. Xuan, Y. Li, X. Guo, J. Zheng, J. Xiao, J. Wu, *J. Mater. Chem. B* **2019**, *7*, 1697.
- [26] Y. Zhu, J. Zhang, J. Song, J. Yang, Z. Du, W. Zhao, H. Guo, C. Wen, Q. Li, X. Sui, L. Zhang, *Adv. Funct. Mater.* **2020**, *30*, 1905493.
- [27] Q. Jiao, L. Cao, Z. Zhao, H. Zhang, J. Li, Y. Wei, *Biomacromolecules* **2021**, *22*, 1220.
- [28] X. Pei, H. Zhang, Y. Zhou, L. Zhou, J. Fu, *Mater. Horiz.* **2020**, *7*, 1872.
- [29] H. Liu, L. Yang, B. Dou, J. Lan, J. Shang, S. Lin, *Sep. Purif. Technol.* **2021**, *279*, 119789.
- [30] S. H. Liu, J. Y. Tang, F. Q. Ji, W. F. Lin, S. F. Chen, *Gels* **2022**, *8*, 46.
- [31] N. Erathodiyil, H. M. Chan, H. Wu, J. Y. Ying, *Mater. Today* **2020**, *38*, 84.
- [32] S. Prieto, A. Shkilnyy, C. Rumpelshaus, A. Ribeiro, F. J. Arias, J. C. Rodríguez-Cabello, A. Taubert, *Biomacromolecules* **2011**, *12*, 1480.
- [33] A. Shkilnyy, R. Gräf, B. Hiebl, A. T. Neffe, A. Friedrich, J. Hartmann, A. Taubert, *Macromol. Biosci.* **2009**, *9*, 179.
- [34] M. Schneider, C. Gunter, A. Taubert, *Polymers* **2018**, *10*, 275.
- [35] T. Mai, K. Wolski, A. Puciul-Malinowska, A. Kopyshv, R. Graf, M. Bruns, S. Zapotoczny, A. Taubert, *Polymers* **2018**, *10*, 1165.
- [36] R. B. J. Ihlenburg, A. C. Lehnen, J. Koetz, A. Taubert, *Polymers* **2021**, *13*, 208.
- [37] R. B. J. Ihlenburg, T. Mai, A. F. Thünemann, R. Baerenwald, K. Saalwächter, J. Koetz, A. Taubert, *J. Phys. Chem. B* **2021**, *125*, 3398.

- [38] H. Y. Kim, R. Y. K. Chang, S. Morales, H. K. Chan, *Antibiotics* **2021**, *10*, 130.
- [39] I. M. Martins, R. L. Reis, H. S. Azevedo, *ACS Chem. Biol.* **2016**, *11*, 2962.
- [40] G. P. Smith, *Science* **1985**, *228*, 1315.
- [41] D. Marvin, *Curr. Opin. Struct. Biol.* **1998**, *8*, 150.
- [42] G. Å. Løset, I. Sandlie, *Methods* **2012**, *58*, 40.
- [43] S. Kilper, T. Jahnke, K. Wieggers, V. Grohe, Z. Burghard, J. Bill, D. Rothenstein, *Materials* **2019**, *12*, 904.
- [44] D. Rothenstein, B. Claasen, B. Omiecienski, P. Lammel, J. Bill, *J. Am. Chem. Soc.* **2012**, *134*, 12547.
- [45] D. Rothenstein, D. Shopova-Gospodinova, G. Bakradze, L. P. H. Jeurgens, J. Bill, *CrystEngComm* **2015**, *17*, 1783.
- [46] H. Heinz, B. L. Farmer, R. B. Pandey, J. M. Slocik, S. S. Patnaik, R. Pachter, R. R. Naik, *J. Am. Chem. Soc.* **2009**, *131*, 9704.
- [47] D. Rothenstein, S. J. Facey, M. Ploss, P. Hans, M. Melcher, V. Srot, P. A. v. Aken, B. Hauer, J. Bill, *Bioinspired, Biomimetic Nanobiomater.* **2013**, *2*, 173.
- [48] S. Kilper, S. J. Facey, Z. Burghard, B. Hauer, D. Rothenstein, J. Bill, *Adv. Funct. Mater.* **2018**, *28*, 1705842.
- [49] S. Kilper, T. Jahnke, M. Aulich, Z. Burghard, D. Rothenstein, J. Bill, *Adv. Mater.* **2019**, *31*, 1805597.
- [50] M. Adhikari, S. Dhamane, A. E. V. Hagström, G. Garvey, W.-H. Chen, K. Kourentzi, U. Strych, R. C. Willson, *Analyst* **2013**, *138*, 5584.
- [51] M. Adhikari, U. Strych, J. Kim, H. Goux, S. Dhamane, M.-V. Poongavanam, A. E. V. Hagström, K. Kourentzi, J. C. Conrad, R. C. Willson, *Anal. Chem.* **2015**, *87*, 11660.
- [52] Y. J. Lee, H. Yi, W.-J. Kim, K. Kang, D. S. Yun, M. S. Strano, G. Ceder, A. M. Belcher, *Science* **2009**, *324*, 1051.
- [53] K. T. Nam, R. Wartena, P. J. Yoo, F. W. Liaw, Y. J. Lee, Y.-M. Chiang, P. T. Hammond, A. M. Belcher, *Proc. Natl. Acad. Sci. USA* **2008**, *105*, 17227.
- [54] K. A. Günay, H.-A. Klok, *Bioconjugate Chem.* **2015**, *26*, 2002.
- [55] T. Serizawa, T. Sawada, H. Matsuno, *Langmuir* **2007**, *23*, 11127.
- [56] J. Chen, T. Serizawa, M. Komiyama, *Angew. Chem., Int. Ed.* **2009**, *48*, 2917.
- [57] H. Matsuno, J. Sekine, H. Yajima, T. Serizawa, *Langmuir* **2008**, *24*, 6399.
- [58] T. Date, J. Sekine, H. Matsuno, T. Serizawa, *ACS Appl. Mater. Interfaces* **2011**, *3*, 351.
- [59] C. Juds, J. Schmidt, M. G. Weller, T. Lange, U. Beck, T. Conrad, H. G. Börner, *J. Am. Chem. Soc.* **2020**, *142*, 10624.
- [60] S. Swaminathan, Y. Cui, *RSC Adv.* **2012**, *2*, 12724.
- [61] N. B. Adey, A. H. Mataragnon, J. E. Rider, J. M. Carter, B. K. Kay, *Gene* **1995**, *156*, 27.
- [62] M. H. Caparon, P. A. De Ciechi, C. S. Devine, P. O. Olins, S. C. Lee, *Mol. Diversity* **1996**, *1*, 241.
- [63] M. Vodnik, U. Zager, B. Strukelj, M. Lunder, *Molecules* **2011**, *16*, 790.
- [64] T. Serizawa, H. Fukuta, T. Date, T. Sawada, *Chem. Commun.* **2016**, *52*, 2241.
- [65] H. Ejima, H. Kikuchi, H. Matsuno, H. Yajima, T. Serizawa, *Chem. Mater.* **2010**, *22*, 6032.
- [66] S.-H. Lee, I. Moody, Z. Zeng, E. B. Fleischer, G. A. Weiss, K. J. Shea, *ACS Appl. Bio Mater.* **2021**, *4*, 2704.
- [67] S. Suzuki, T. Sawada, T. Ishizone, T. Serizawa, *Chem. Commun.* **2016**, *52*, 5670.
- [68] A. J. Keefe, K. B. Caldwell, A. K. Nowinski, A. D. White, A. Thakkar, S. Jiang, *Biomaterials* **2013**, *34*, 1871.
- [69] J. Jumper, R. Evans, A. Pritzel, T. Green, M. Figurnov, O. Ronneberger, K. Tunyasuvunakool, R. Bates, A. Žídek, A. Potapenko, A. Bridgland, C. Meyer, S. A. A. Kohl, A. J. Ballard, A. Cowie, B. Romera-Paredes, S. Nikolov, R. Jain, J. Adler, T. Back, S. Petersen, D. Reiman, E. Clancy, M. Zielinski, M. Steinegger, M. Pacholska, T. Berghammer, S. Bodenstein, D. Silver, O. Vinyals, et al., *Nature* **2021**, *596*, 583.
- [70] D. Case, V. Babin, J. Berryman, R. Betz, Q. Cai, D. Cerutti, T. Cheatham, III, T. Darden, R. Duke, H. Gohlke, AMBER 14; University of California: San Francisco **2014**, 1–826.
- [71] V. Mariani, M. Biasini, A. Barbato, T. Schwede, *Bioinformatics* **2013**, *29*, 2722.
- [72] E. Jurrus, D. Engel, K. Star, K. Monson, J. Brandi, L. E. Felberg, D. H. Brookes, L. Wilson, J. Chen, K. Liles, M. Chun, P. Li, D. W. Gohara, T. Dolinsky, R. Konecny, D. R. Koes, J. E. Nielsen, T. Head-Gordon, W. Geng, R. Krasny, G.-W. Wei, M. J. Holst, J. A. Mccammon, N. A. Baker, *Protein Sci.* **2018**, *27*, 112.
- [73] W. L. DeLano, *The PyMOL Molecular Graphics System*, Palo Alto, CA, USA **2018**.
- [74] M. L. Lemloh, K. Altintoprak, C. Wege, I. M. Weiss, D. Rothenstein, *Materials* **2017**, *10*, 119.
- [75] T. Iwasaki, M. Maruyama, T. Niwa, T. Sawada, T. Serizawa, *Polym. J.* **2021**, *53*, 1439.
- [76] T. J. Dolinsky, J. E. Nielsen, J. A. Mccammon, N. A. Baker, *Nucleic Acids Res.* **2004**, *32*, W665.
- [77] M. H. M. Olsson, C. R. Søndergaard, M. Rostkowski, J. H. Jensen, *J. Chem. Theory Comput.* **2011**, *7*, 525.